*Kovove Mater. 49 2011 85–92*
*DOI: 10.4149/km_2011_1_85*



# Fabrication of ultrafine-grained Ti-(5–50wt.%)$Al_2O_3$ composites using high-pressure torsion

K. Edalati[1]*, H. Iwaoka[1], Z. Horita[1], M. Tanaka[1], K. Higashida[1], H. Fujiwara[2], K. Ameyama[3]

[1] *Department of Materials Science and Engineering, Faculty of Engineering, Kyushu University, Fukuoka 819-0395, Japan*
[2] *Ritsumeikan Global Innovation Research Organization, Ritsumeikan University, Kusatsu 525-8577, Japan*
[3] *Department of Materials Science and Engineering, Faculty of Science and Engineering, Ritsumeikan University, Kusatsu 525-8577, Japan*

Received 21 July 2010, received in revised form 13 August 2010, accepted 20 August 2010

**Abstract**

Ti-matrix composites reinforced with $Al_2O_3$ fractions of up to 50 wt.% were fabricated by cold consolidation of powder mixtures using high-pressure torsion (HPT). The grain size of the Ti matrix was reduced to ∼ 100 nm. A relative density greater than ∼ 99 % was attained for composites containing up to 30 % $Al_2O_3$ following the rule of mixture. The Vickers microhardness increased with an increase in the $Al_2O_3$ fraction but the bending stress and ductility decreased. The HPT-processed composites exhibited an abrupt increase in the hardness when they were annealed at 800–900 K, indicating a successful achievement of consolidation.

K e y w o r d s: titanium, Ti-matrix composite, ultrafine grain, high-pressure torsion, severe plastic deformation, consolidation

## 1. Introduction

Metal-matrix composites have been the subject of scientific investigation for a few decades and they have been used as high performance materials in various engineering applications in recent years [1]. Among metal-matrix composites, Ti-matrix composites with ceramic reinforcements are of particular interest [2]. The greatest potential of Ti-matrix composites lies in their high strength to weight ratio and good high temperature properties [2, 3]. Ti-$Al_2O_3$ composites are considered as promising candidates for aeronautical and automobile applications [2, 3]. Additionally, Ti-$Al_2O_3$ composites may be considered as favorable materials for biomedical applications because of their high biocompatibility and the excellent mechanical properties of both Ti and $Al_2O_3$ constituents [4].

Fabrication of Ti-$Al_2O_3$ composites, especially with large fractions of $Al_2O_3$, is difficult using conventional techniques such as hot-press sintering because of the high sintering temperature and long sintering time [5]. On the one hand, the high sintering temperature and long sintering time lead to interfacial reaction of Ti and $Al_2O_3$ and result in producing brittle intermetallics [5]. On the other hand, large residual stress and microcracks are formed in the interface because of thermal expansion mismatch between Ti and $Al_2O_3$ [6]. To avoid the sintering problems, cold consolidation using the high pressure torsion (HPT) method might be an effective solution.

In the HPT method, a thin disc specimen is placed between two massive anvils under high pressure and intense shear is introduced by rotating the two massive anvils with respect to each other [7]. The HPT method is usually used to achieve ultrafine grained materials at the nanometer or sub-micrometer level [8, 9]. In addition to grain refinement, the HPT is also applicable as a processing tool for consolidation of metallic powders [10–12], ceramic powders [13] and metallic and amorphous machining chips [14, 15] without sintering process. The application also includes the cold consolidation of composite powders such as Al-5 and 15vol.%$Al_2O_3$ [16, 17], Al-5 and 15vol.%SiC [16], Al-5% carbon nanotubes (all compositions are weight percentages unless otherwise indicated) [18], Al-5% fullerene [19], Cu-0.5%$Al_2O_3$ [20, 21], Cu-5vol.%$SiO_2$

*Corresponding author: tel./fax: +81-92-802-2992; e-mail address: kaveh.edalati@zaiko6.zaiko.kyushu-u.ac.jp

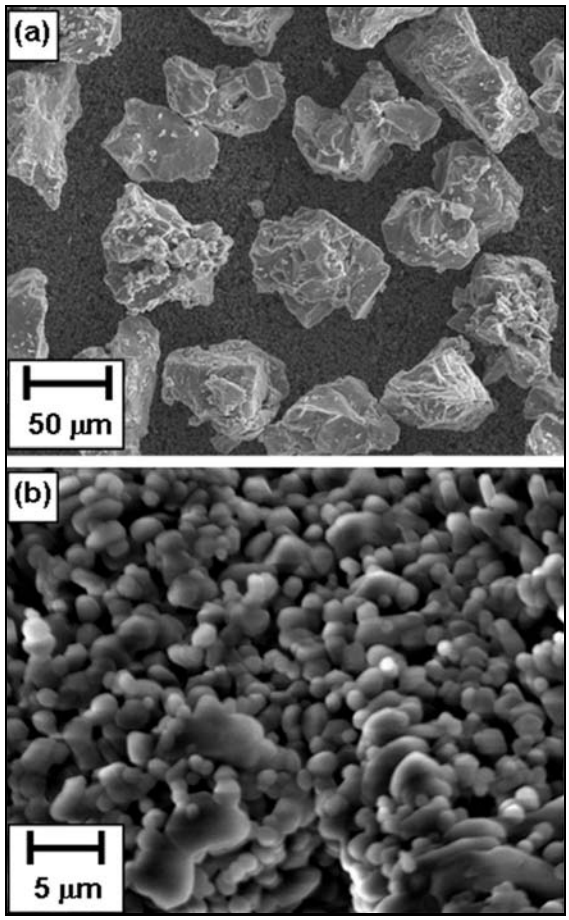


Fig. 1. Morphology of (a) Ti powders and (b) $Al_2O_3$ powders observed using scanning electron microscopy.

[16, 17], Cu-1% carbon nanotubes [22, 23], Ti-5 and 10vol.%$TiO_2$ [24], Co-50%NiO [25], Co-5 to 50%$Al_2O_3$ [27] and $Al_{84}Y_3Ni_8Co_4Zr_1$-SiC [27]. Menendez et al. [27] used ball milling followed by HPT for consolidation of $Al_2O_3$ reinforced Co-matrix composites with large fractions of $Al_2O_3$ from 5 to 50 % and found that the nanocomposites were consolidated satisfactorily for up to 20 % of $Al_2O_3$.

In this study, and for the first time, Ti-$Al_2O_3$ powder mixtures with large fraction of $Al_2O_3$ (from 0 to 50 %) are subjected to HPT for two main objectives: one is to consolidate the composites without the sintering process and the other is to produce composites with ultrafine-grained structures.

## 2. Experimental procedures

Materials used in this study were high purity Ti (99.9 %) powders with ∼ 70 μm diameter and commercially pure $\alpha$-$Al_2O_3$ powders with ∼ 1 μm particle size. The morphology of Ti and $Al_2O_3$ powders taken by a scanning electron microscope is shown in Fig. 1a and 1b, respectively. The Ti powders were mixed with either 0, 5, 10, 20, 30 or 50 % (in wt.%) of the $Al_2O_3$ powders using mechanical agitation. As a reference material, a rod of pure Ti (99.9 %) with 10 mm diameter and 70 mm length was also used in this study. The rod was annealed for 1 hour at 1073 K under an argon atmosphere and sliced to discs with thicknesses of 0.85 mm using a wire-cutting electric discharge machine. The HPT facility consists of upper and lower anvils having a shallow hole of 10 mm diameter and 0.25 mm depth at the center. A bulk disc or ∼ 0.5 g of the powder mixtures was put in the hole located at the center of the lower anvil. HPT was then conducted at room temperature at a rotation speed of $\omega = 1$ rpm for $N = 10$ revolutions under a pressure of $P = 6$ GPa. The details concerning the HPT facility have been reported elsewhere [28].

The HPT-processed samples were annealed at a selected temperature in the range of 573 K to 1273 K for 1 hour in an argon atmosphere. All samples were evaluated through measurements of density, Vickers microhardness and bending properties and were analyzed by optical microscopy (OM), transmission electron microscopy (TEM) and X-ray diffraction (XRD).

First, after processing by HPT, disc samples were polished to a mirror-like surface and the microstructures of samples were observed using OM.

Second, disc samples were polished to a mirror-like surface on both sides and the sample density was determined by Archimedes' principle using an electronic balance with an accuracy of 0.1 mg, as described in details in an earlier paper [29].

Third, the Vickers microhardness was measured at every 1 mm from the center to edge in 8 radial directions using an applied load of 1 kg for duration of 15 s.

Fourth, miniature rods with a 0.5 mm square cross section and 9 mm length for bending tests were cut from discs at 1 mm from the disc center. Three-point bending tests were carried out at room temperature to measure the bending load and displacement of samples. The supporting span was 8 mm and the stroke was controlled at a cross-head speed of 0.5 mm $s^{-1}$. The bending stress was calculated from the load and the specimen geometry, as described elsewhere [30].

Fifth, for TEM, 3 mm discs were punched out from the HPT-processed discs at 3.5 mm from the center and ground mechanically to a thickness of 0.15 mm and further thinned with a twin-jet electrochemical polisher using a solution of 4vol.%$HClO_4$, 25vol.%$C_3H_3(CH_2)_2CH_2OH$ and 71vol.%$CH_3OH$ at 263 K under an applied voltage of 10 V. TEM was performed at 200 kV for microstructural observation and for recording selected-area electron diffraction (SAED) patterns.

Sixth, structural analyses with XRD were per-

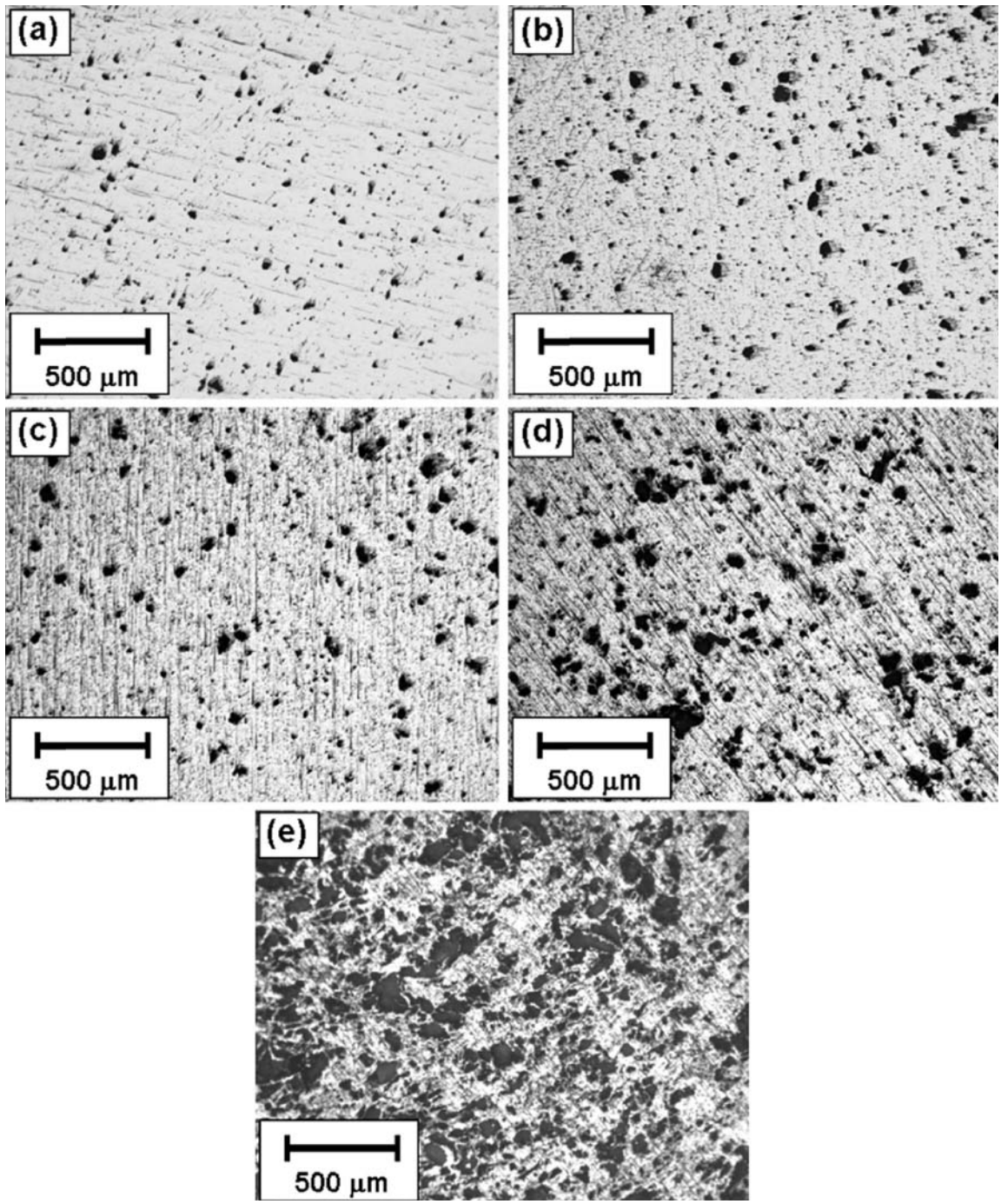


Fig. 2. Micrographs of HPT-processed samples containing (a) 5, (b) 10, (c) 20, (d) 30 and (e) 50 % $Al_2O_3$ observed using optical microscopy.

formed using the Co K$\alpha$ radiation at 50 kV and 30 mA in scanning step of 0.02° and scanning speed of 2°/min.

## 3. Results and discussion

OM micrographs are shown in Fig. 2a to 2e for the HPT-processed samples containing 5, 10, 20, 30 and 50 % $Al_2O_3$, respectively. The dark areas correspond to $Al_2O_3$ particles and it is apparent that they increase with increasing fraction of $Al_2O_3$. There are many dark areas sizes of which are larger than the size of $\sim 70$ μm visible in Fig. 2e. This indicates that many fractions of the $Al_2O_3$ particles are present in an agglomerated form.

Figure 3 plots the variation of (a) density and (b) relative density as a function of the $Al_2O_3$ fraction

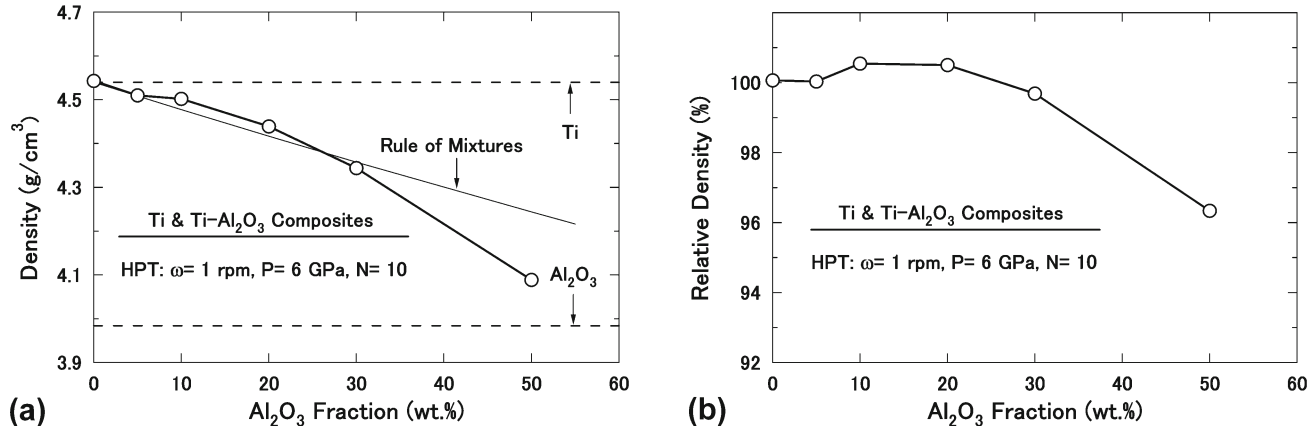


Fig. 3. Variations of (a) density and (b) relative density as a function of $Al_2O_3$ fraction for Ti-$Al_2O_3$ composites consolidated with HPT. Rule of mixtures and density levels of Ti and $Al_2O_3$ are delineated.

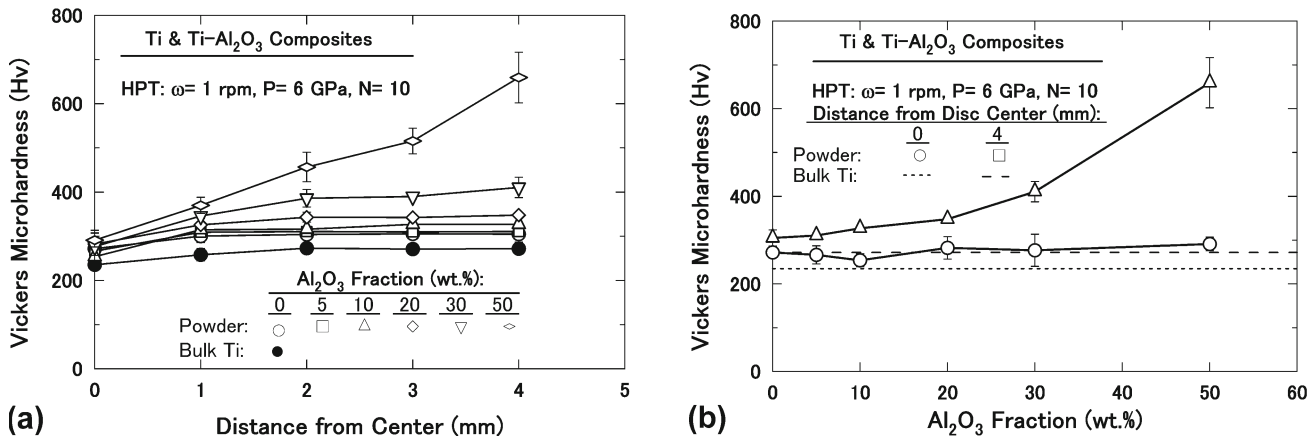


Fig. 4. Variations of Vickers microhardness (a) plotted along distance from disc center after consolidation with HPT and (b) plotted against $Al_2O_3$ fraction at disc center and 4 mm from disc center including hardness levels for bulk Ti at corresponding positions.

for the samples consolidated with HPT. In Fig. 3a, the two dashed lines represent the density of pure Ti ($4.54\,g\,cm^{-3}$) [31] and that of $Al_2O_3$ ($3.984\,g\,cm^{-3}$) [32] and the rule of mixtures is delineated by a solid line. It is found that the measured density decreases monotonically with an increase in the fraction of $Al_2O_3$. This decrease is well consistent with the rule of mixtures up to the $Al_2O_3$ fraction of $\sim$ 30 % but an appreciable deviation occurs to a lower level above the fraction of $\sim$ 30 %. It is thus concluded that the former decrease in density can be attributed to the lower density of $Al_2O_3$ and the later decrease can be due to poor consolidation of the composite. This conclusion is well documented in Fig. 3b when the relative density is plotted against the fraction of $Al_2O_3$. The relative density is almost 100 % for the $Al_2O_3$ fraction of up to $\sim$ 30 % but decreases to $\sim$ 95 % for the composite containing 50 % of $Al_2O_3$. Nevertheless, the relative density achieved after cold consolidation with HPT for the 50%$Al_2O_3$ composite is comparable with those of other consolidation methods such as hot-press sintering and is higher than those reported by Menendez et al. [27] for consolidation of $Al_2O_3$ reinforced Co-matrix composites with fractions of $Al_2O_3$ from 5 to 50 %.

Figure 4a shows the variation of microhardness along the distance from the disc center for the five different fractions of $Al_2O_3$ after consolidation with HPT. The hardness variation for the samples without $Al_2O_3$ is also included in Fig. 4a. In Fig. 4b, the hardness is plotted against the $Al_2O_3$ fraction and a comparison is made between the hardness at the disc center and the hardness at the position 4 mm from the disc center. The two hardness levels are also shown from the bulk Ti at the corresponding positions.

In Fig. 4a, the hardness increases with the distance from the disc center. This increase becomes prominent as the $Al_2O_3$ fraction increases. Whereas the hardness saturates to constant levels for the samples containing the $Al_2O_3$ fractions of up to 30 %, the hardness keeps increasing with the distance from the center for the sample with the 50%$Al_2O_3$ fraction. This trend is

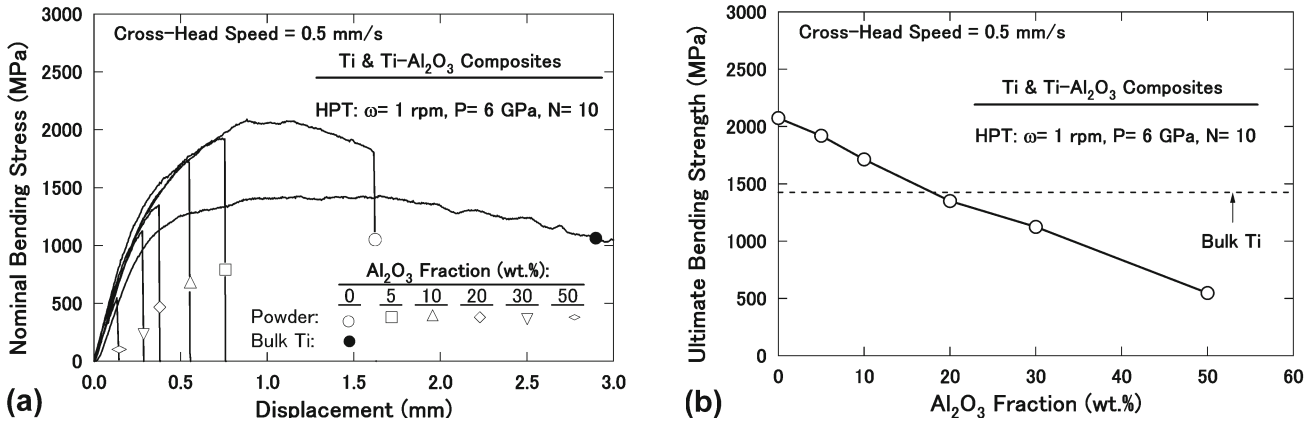


Fig. 5. (a) Stress-displacement curves obtained from bending tests and (b) ultimate bending strength plotted against $Al_2O_3$ fraction. Results of powder Ti and bulk Ti processed with HPT are included.

more clearly demonstrated in Fig. 4b, where the hardness increase is little at the center but it is significant for the position 4 mm from the disc center.

The hardness increase with the distance from the center can be attributed to an increase in strain. The equivalent strain, $\varepsilon$, for HPT is estimated as [9]:

$$\varepsilon = \frac{r\theta}{\sqrt{3}t}, \tag{1}$$

where $r$ is the distance from the disc center, $\theta$ is the rotation angle in radian and $t$ is the thickness of the disc. It should be noted that the real strain introduced in the sample is calculated using the equation as described earlier [33] where the effect of slippage and thickness reduction during HPT was taken into account. The equation indicates that the strain is theoretically zero at the center of the disc and increases with an increase in the distance from the center. Therefore, consolidation and grain refinement occur as a strain-assisted process and thus the hardness increases with an increase in the distance from the disc center as shown in Fig. 4a. These observations are well consistent with our earlier reports concerning the consolidation of ball-milled Ti powders [29], of ceramics [13] and of amorphous chips [15] using HPT. In addition to the effect of strain, the hardness increases with an increase in the fraction of $Al_2O_3$ and this is because $Al_2O_3$ is known to be much harder than Ti.

The hardness saturation in the composites containing the $Al_2O_3$ fractions of up to $\sim$ 30 % appears not only because a full consolidation is achieved by the HPT processing but also because a balance is reached between the hardening by straining and the softening by recovery and/or recrystallization during the HPT processing as described for pure metals [33, 34]. The continuous increase in the hardness with strain for the composite containing 50%$Al_2O_3$ arises because imposed strain is insufficient to attain not only a full consolidation but also a homogeneous distribution of the $Al_2O_3$ particles within the HPT processing for 10 revolutions.

Figure 5 shows (a) the stress-displacement curves obtained from bending tests and (b) the maximum bending stress plotted against the $Al_2O_3$ fraction. For comparison, the results of powder Ti and bulk Ti processed with HPT are included in Fig. 5. The increasing fraction of $Al_2O_3$ leads to the decrease in the maximum bending stress and the displacement to the fracture decreases with the increasing fraction of $Al_2O_3$. This trend is different from the one obtained by the hardness measurement shown in Fig. 4b. It is considered that the opposite trend arises because the testing principle is different: while the hardness measurement may be less affected by the connectivity at the interface between the particle and the matrix, the effect should be large in the bending test especially at the tension side of the specimen. Although the consolidation by HPT is high to increase the density, the connectivity at the interface between the particle and the matrix may not be sufficient.

A close inspection of Figs. 4 and 5 reveals that the hardness and the bending strength after processing with HPT for Ti powders are invariably higher than those for bulk Ti despite the same impurity level. This is consistent with an earlier report [29] and it can be due to the presence of oxide layers on the surfaces of Ti powders which act as a reinforcement.

TEM microstructures of a bright-field image and a dark-field image including a corresponding SAED pattern are shown in Fig. 6a to 6c, respectively, for the composite containing 5 % of $Al_2O_3$. Note that the dark-field images were taken with the diffracted beam indicated by an arrow in the SAED pattern. It is apparent that the microstructure consists of small grains at the nanometer or sub-micrometer level. The average grain size measured for 20 grains appears to be $\sim$ 100 nm, which is smaller than the value reported earlier for bulk Ti after processing with HPT [28]. The microstructural features are very similar to earlier ob-

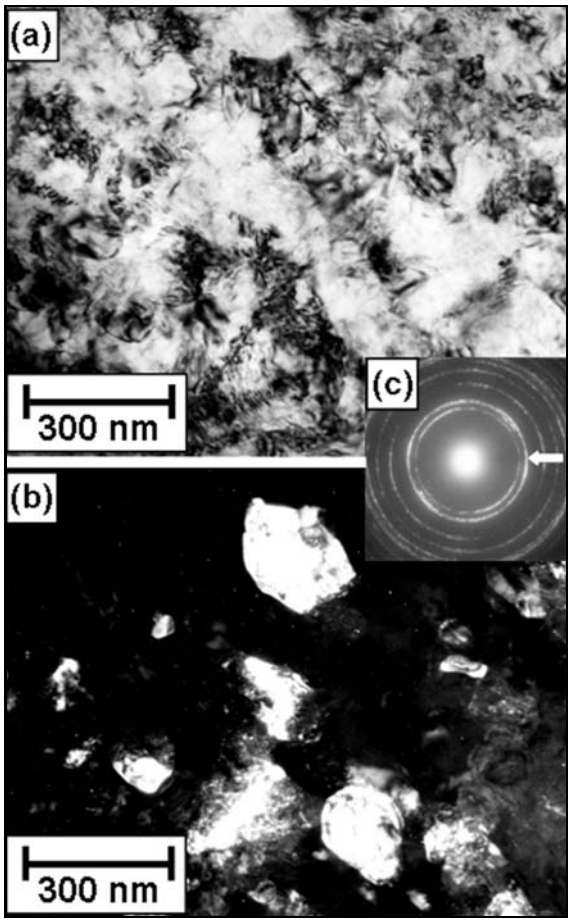


Fig. 6. (a) TEM bright-field image, (b) TEM dark-field image and (c) SAED pattern for Ti-5%$Al_2O_3$ consolidated with HPT. Arrow in SAED pattern indicates diffracted beam for dark-field image.

servations of Ti [28, 29]: there are many dislocations within the grains and the grain boundaries are in high angles of misorientation. It is important to emphasize that producing ultrafine grains in Ti-$Al_2O_3$ composites is essentially difficult using other consolidation methods such as hot-press sintering because of high sintering temperature and long sintering time. Therefore, the HPT provides a unique opportunity for cold-consolidation of Ti-$Al_2O_3$ composites with ultrafine grained structure.

It is known that Ti exhibits a pressure-induced phase transformation from an $\alpha$ phase with the *hcp* crystal structure to an $\omega$ phase with the simple hexagonal structure during HPT under the pressures higher than 4 GPa [29]. The HPT was conducted under 6 GPa in this work, but XRD analysis confirmed that the transformation to $\omega$ phase was not detected because of the rotation speed which was high enough to raise temperature during HPT processing and thus to induce the reverse transformation to $\alpha$ phase.

The composites containing 20 % and 50 % of $Al_2O_3$

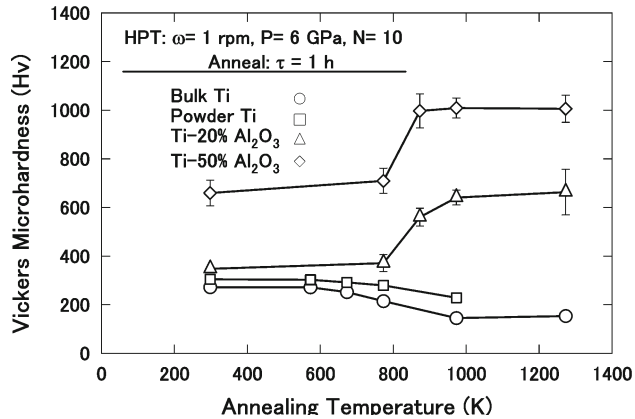


Fig. 7. Variations of Vickers microhardness with respect to annealing temperature for HPT-processed composites containing 20 % and 50 % of $Al_2O_3$ including HPT-processed pure Ti powders and pure Ti bulk.

were annealed for 1 hour at a temperature in the range up to $\sim$ 1273 K. The hardness was measured and plotted in Fig. 7 against the annealing temperature. Figure 7 also includes the hardness variation of HPT-processed Ti powders and Ti bulk for comparison. While the hardness decreases with increasing annealing temperature in both forms of pure Ti, the composites with the two different $Al_2O_3$ fractions exhibit abrupt increases in the hardness around a temperature of 800–900 K. These increases range up to as large as $\sim$ 300 Hv. It is considered that the increases can be attributed to a formation of a reaction product, $Ti_3Al$, as reported by Misra [35] and Zalar et al. [36]. Although detailed microstructural analysis is now in progress, the increase in the hardness should be reasonable because the reaction product, $Ti_3Al$, is an intermetallic phase with high strength.

## 4. Conclusions

Ti-$Al_2O_3$ composites with the $Al_2O_3$ fraction of up to 50 wt.% were cold-consolidated by high-pressure torsion (HPT) and the following conclusions were obtained:

1. Composites containing up to $\sim$ 30 % $Al_2O_3$ can be consolidated with a relative density greater than $\sim$ 99 % following the rule of mixtures. The consolidation is lowered for the composite containing 50 % $Al_2O_3$ so that the relative density decreases to 95 %.

2. TEM examinations confirm that the microstructure of the Ti matrix consists of ultrafine grains with the grain size of $\sim$ 100 nm.

3. The hardness increases with increasing fraction of $Al_2O_3$ but by contrast both bending stress and displacement to fracture decrease.

4. There are abrupt increases in hardness when the

composites consolidated by HPT are annealed at 800–900 K.

## Acknowledgements

We would like to thank Prof. H. Miura of Kyushu University for providing a facility for density measurement. One of the authors (K.E.) thanks the Islamic Development Bank for its support through a scholarship. This work was supported in part by a Grant-in-Aid for Scientific Research from the Ministry of Education, Culture, Sports, Science and Technology of Japan in the Priority Area "Giant Straining Process for Advanced Materials Containing Ultra-High Density Lattice Defects" and in part by Kyushu University Interdisciplinary Programs in Education and Projects in Research Development (P&P).

## References

[1] MATTHEWS, F. L.—RAWLINGS, R. D.: Composite Materials – Engineering and Science. Cambridge, Woodhead Publishing Limited 2003.
[2] VASSEL, A.: Mater. Sci. Eng. A, *263*, 1999, p. 305. doi:10.1016/S0921-5093(98)01161-7
[3] MAS-GUINDAL, M. J.—BENKO, E.—RODRIGUEZ, M. A.: J. Alloys Compd., *454*, 2008, p. 352. doi:10.1016/j.jallcom.2006.12.105
[4] GIBBESCH, B.—ELSSNER, G.—PETZOW, G.: Clin. Mater., *5*, 1990, p. 177. doi:10.1016/0267-6605(90)90017-P
[5] ZHI, W.—KUN, X.—QIANG, S.—YINGZI, W.—LIANMENG, Z.: Journal of Wuhan University of Technology – Mater. Sci. Ed., *20*, 2005, p. 30.
[6] HOUGH, H.—DEMAS, J.—WILLIAMS, T. O.—WADLEY, H. N. G.: Acta Metall. Mater., *43*, 1995, p. 821. doi:10.1016/0956-7151(94)00281-L
[7] BRIDGMAN, P. W.: Phys. Rev., *48*, 1935, p. 825. doi:10.1103/PhysRev.48.825
[8] ZHILYAEV, A. P.—LANGDON, T. G.: Prog. Mater. Sci., *53*, 2008, p. 893. doi:10.1016/j.pmatsci.2008.03.002
[9] VALIEV, R. Z.—ESTRIN, Y.—HORITA, Z.—LANGDON, T. G.—ZEHETBAUER, M. J.—ZHU, Y. T.: JOM, *58*, 2006, p. 33.
[10] KORZNIKOV, A. V.—SAFAROV, I.—LAPTIONOK, D. V.—VALIEV, R. Z.: Acta Metal. Mater., *39*, 1991, p. 3193.
[11] SHEN, H.—GUENTHER, B.—KOANIKOV, A. V.—VALIEV, R. Z.: Nanostruct. Mater., *6*, 1995, p. 385. doi:10.1016/0965-9773(95)00077-1
[12] EDALATI, K.—HORITA, Z.—FUJIWARA, H.—AMEYAMA, K.—TANAKA M.—HIGASHIDA, K.: Mater. Sci. Forum, *654–656*, 2010, p. 1239. doi:10.4028/www.scientific.net/MSF.654-656.1239
[13] EDALATI, K.—HORITA, Z.: Scripta Mater., *63*, 2010, p. 174.
[14] ZHILYAEV, A. P.—GIMAZOV, A. A.—RAAB, G. I.—LANGDON, T. G.: Mater. Sci. Eng. A, *486*, 2008, p. 123. doi:10.1016/j.msea.2007.08.070
[15] EDALATI, K.—YOKOYAMA, Y.—HORITA, Z.: Mater. Trans., *51*, 2010, p. 23. doi:10.2320/matertrans.MB200914
[16] ALEXANDROV, I. V.—ZHU, Y. T.—LOWE, T. C.—ISLAMGALIEV, R. K.—VALIEV, R. Z.: Nanostruct. Mater., *10*, 1998, p. 45. doi:10.1016/S0965-9773(98)00026-9
[17] ALEXANDROV, I. V.—ZHU, Y. T.—LOWE, T. C.—ISLAMGALIEV, R. K.—VALIEV, R. Z.: Metall. Mater. Trans. A, *29*, 1998, p. 2253. doi:10.1007/s11661-998-0103-4
[18] TOKUNAGA, T.—KANEKO, K.—HORITA, Z.: Mater. Sci. Eng. A, *490*, 2008, p. 300. doi:10.1016/j.msea.2008.02.022
[19] TOKUNAGA, T.—KANEKO, K.—SATO, K.—HORITA, Z.: Scripta Mater., *58*, 2008, p. 735. doi:10.1016/j.scriptamat.2007.12.010
[20] KUZEL, R.—MATEJ, Z.—CHERKASKA, V.—PESICKA, J.—CIZEK, J.—PROCHAZKA, I.—ISLAMGALIEV, R. K.: J. Alloys Compd., *378*, 2004, p. 242.
[21] ISLAMGALIEV, R. K.—BUCHGRABER, W.—KOLOBOV, Y. R.—AMIRKHANOV, N. M.—SERGUEEVA, A. V.—IVANOV, K. V.—GRABOVETSKAYA, G. P.: Mater. Sci. Eng. A, *319–321*, 2001, p. 872. doi:10.1016/S0921-5093(01)01073-5
[22] LI, H.—MISRA, A.—ZHU, Y.—HORITA, Z.—KOCH, C. C.—HOLESINGER, T. G.: Mater. Sci. Eng. A, *523*, 2009, p. 60. doi:10.1016/j.msea.2009.05.031
[23] LI, H.—MISRA, A.—HORITA, Z.—KOCH, C. C.—MARA, N. A.—DICKERSON, P. O.—HU, Y.: J. Appl. Phys., *95*, 2009, p. 071907.
[24] STOLYAROV, V. V.—ZHU, Y. T.—LOWE, T. C.—ISLAMGALIEV, R. K.—VALIEV, R. Z.: Mater. Sci. Eng. A, *282*, 2000, p. 78. doi:10.1016/S0921-5093(99)00764-9
[25] MENENDEZ, E.—SORT, J.—LANGLAIS, V.—ZHILYAEV, A.—MUNOZ, J. S.—SURINACH, S.—NOGUES, J.—BARO, M. D.: J. Alloys Compd., *434–435*, 2007, p. 505. doi:10.1016/j.jallcom.2006.08.135
[26] BOTTA-FILHO, W. J.—FOGAGNOLO, J. B.—RODRIGUES, C. A. D.—KIMINAMI, C. S.—BOLFARINI, C.—YAVARI, A. R.: Mater. Sci. Eng. A, *375–377*, 2004, p. 936. doi:10.1016/j.msea.2003.10.072
[27] MENENDEZ, E.—SALAZAR-ALVAREZ, G.—ZHILYAEV, A. P.—SURINACH, S.—BARO, M. D.—NOGUES, J.—SORT, J.: Adv. Funct. Mater., *18*, 2008, p. 3293. doi:10.1002/adfm.200800456
[28] EDALATI, K.—MATSUBARA, E.—HORITA, Z.: Metall. Mater. Trans. A, *40*, 2009, p. 2079. doi:10.1007/s11661-009-9890-5
[29] EDALATI, K.—HORITA, Z.—FUJIWARA, H.—AMEYAMA, K.: Metall. Mater. Trans. A, 2010 (in press).
[30] ASTM E290: Standard Test Methods for Bend Testing of Material for Ductility. ASTM International, West Conshohocken, PA 2009.
[31] EMSLEY, J.: The Elements. Oxford, Clarendon Press 1991.
[32] RAO, P.—IWASA, M.—KONDOH, I.: J. Mater. Sci. Lett., *19*, 2000, p. 543. doi:10.1023/A:1006753522757
[33] EDALATI, K.—FUJIOKA, T.—HORITA, Z.: Mater. Trans., *50*, 2009, p. 44.

[34] EDALATI, K.—FUJIOKA, T.—HORITA, Z.: Mater. Sci. Eng. A, *497*, 2008, p. 168. doi:10.1016/j.msea.2008.06.039

[35] MISRA, A. K.: Metall. Trans. A, *22,* 1991, p. 715. doi:10.1007/BF02670294

[36] ZALAR, A.—BARETZKY, B. M. M.—HOFMANN, S.—RUHLE, M.—PANJAN, P.: Thin Solid Films, *352*, 1999, p. 151. doi:10.1016/S0040-6090(99)00352-1